JOURNAL OF VIROLOGY, Apr. 2009, p. 3450–3462 Vol. 83, No. 8
0022-538X/09/$08.00+0 doi:10.1128/JVI.02561-08

Novel Immunocompetent Murine Tumor Model for Evaluation of Conditionally Replication-Competent (Oncolytic) Murine Adenoviral Vectors[▽]

Michael Robinson,[1]* Betty Li,[1] Ying Ge,[1] Derek Ko,[1] Satya Yendluri,[1] Thomas Harding,[1] Melinda VanRoey,[1] Katherine R. Spindler,[2] and Karin Jooss[1]

Cell Genesys, Inc., 500 Forbes Blvd., South San Francisco, California 94080,[1] and Department of Microbiology & Immunology, University of Michigan Medical School, 1150 W. Medical Center Dr., 6724 Medical Science II, Ann Arbor, Michigan 48109-5620[2]

Received 11 December 2008/Accepted 26 January 2009

Oncolytic adenoviral vectors that express immunostimulatory transgenes are currently being evaluated in clinic. Preclinical testing of these vectors has thus far been limited to immunodeficient xenograft tumor models since human adenoviruses do not replicate effectively in murine tumor cells. The effect of the immunostimulatory transgene on overall virus potency can therefore not be readily assessed in these models. Here, a model is described that allows the effective testing of mouse armed oncolytic adenovirus (MAV) vectors in immunocompetent syngeneic tumor models. These studies demonstrate that the MAV vectors have a high level of cytotoxicity in a wide range of murine tumor cells. The murine oncolytic viruses were successfully armed with murine granulocyte-macrophage colony-stimulating factor (mGM-CSF) by a novel method which resulted in vectors with a high level of tumor-specific transgene expression. The mGM-CSF-armed MAV vectors showed an improved level of antitumor potency and induced a systemic antitumor immune response that was greater than that induced by unarmed parental vectors in immunocompetent syngeneic tumor models. Thus, the oncolytic MAV-1 system described here provides a murine homolog model for the testing of murine armed oncolytic adenovirus vectors in immunocompetent animals. The model allows evaluation of the impact of virus replication and the host immune response on overall virus potency and enables the generation of translational data that will be important for guiding the clinical development of these viruses.

Oncolytic adenoviral vectors are currently being developed for the treatment of various cancers (1, 5, 33). The preclinical characterization of oncolytic adenoviral vectors has so far been restricted to immunodeficient xenograft tumor models (29, 31, 49) because human adenoviruses do not replicate efficiently in murine tumor cells (15, 22, 55). While these immunodeficient animal models can demonstrate effective replication in and destruction of human tumors by adenovirus type 5 (Ad5)-based vectors, the viruses do not replicate in mouse tissues and the models thus cannot assess the complete safety and efficacy profile of the vectors in normal tissue, nor do they permit evaluation of the impact of an active immune system on overall vector potency. In contrast, the effect of virus replication and the immune response could be evaluated in an immunocompetent syngeneic tumor model, which is especially important when such viruses are armed with immunomodulatory transgenes to increase their potency. In this report, we describe the use of a species-specific mouse armed oncolytic adenovirus type 1 (MAV-1) vector that can replicate in murine cells (25) as a murine virus homolog to the human oncolytic adenoviruses. MAV-1 is a 31-kb double-stranded DNA virus that has a genomic structure and organization comparable to those of human Ad5 (37, 59), and it has previously been used in an in vivo experimental model to study adenovirus replication in an immunocompetent host (36, 40).

MAV-1 has important similarities and differences with respect to human adenovirus, in terms of both pathogenesis and molecular biology. Both human adenoviruses and MAV-1 cause persistent infections accompanied by sporadic excretion of virus (19, 52, 57, 62). Severe human adenovirus infections occur in people with immunodeficiencies due to infection or immunosuppression, including AIDS patients and transplant recipients (6, 8, 18, 34). MAV-1 also causes morbidity and mortality in immunocompromised hosts (44, 45). For most human adenovirus serotypes, replication is thought to occur first in respiratory epithelium, with most evidence of infection in the eyes and pharynx (66). In contrast, MAV-1 infects primarily endothelial cells throughout the animal; the highest levels of virus are seen in the brain, spinal cord, and spleen (11, 23, 32, 35, 44). MAV-1 also infects respiratory epithelium (64). MAV-1 does not use CAR, the primary attachment receptor used by many human adenoviruses (39). However, cellular α_v integrin and heparan sulfate are receptors for MAV-1 (48), as is the case for human Ad2 and Ad5 (13, 14, 65). It is not known whether α_v integrin and heparan sulfate are used for MAV-1 attachment, entry, or both. Early region 3 (E3) of MAV-1 does not have sequence similarity to E3 of other adenoviruses; it encodes a peripheral membrane protein produced in wild-type virus-infected cells (4). Like other adenovirus E3s, it contributes to pathogenesis (3, 10). A mutant virus lacking E3 elicits reduced inflammatory responses (L. E. Gralinski, S. L. Ashley, S. D. Dixon, and K. R. Spindler, unpublished data; 10), oppo-

* Corresponding author. Mailing address: Cell Genesys, Inc., 500 Forbes Blvd., South San Francisco, CA 94080. Phone: (415) 746-1511. Fax: (415) 512-7022. E-mail: michrobinson@gmail.com.

▽ Published ahead of print on 4 February 2009.

site to results obtained by the deletion of E3 in human adenoviruses (reviewed in reference 54). Despite these differences from human adenoviruses, use of MAV-1 in mice provides an adenovirus model in which physiological doses of virus can be studied in the homologous host.

The MAV-1 E1A protein contains three conserved regions (CR1, CR2, and CR3) that are comparable to the conserved regions found in Ad5 E1A (2). Similar to human adenovirus E1A, MAV-1 E1A interacts with a component of the Mediator complex, Med23 (formerly known as Sur2) (17) and members of the pRB family (17, 58). In the present study, the oncolytic properties of the CR2 deletion-containing MAV-1 vector *dl*E102 were determined. This vector is homologous to the Δ24 oncolytic Ad5 vector, which also contains a deletion in the CR2 region and has been shown to replicate selectively in murine tumor cells that are defective in the *pRb* pathway (21). The *dl*E102 virus was shown to replicate and to have potent antitumor activity in a panel of murine tumor cell lines. In contrast, its replication was attenuated in untransformed murine cells to a degree comparable to the level of attenuation observed with Ad5-based oncolytic vectors in nontransformed human fibroblasts. Furthermore, *dl*E102 demonstrated antitumor activity in vivo in immunocompetent xenograft tumor models. Lastly, this study showed that the potency of *dl*E102 could be increased further by arming it with the immunomodulatory murine cytokine granulocyte-macrophage colony-stimulating factor (mGM-CSF). In this case, a novel approach was used to arm the adenoviral vectors with the murine GM-CSF gene by using the furin and 2A cleavage sequences (16) that link the expression of a transgene to an endogenous viral gene without requiring the addition of large exogenous transcriptional control regions. By utilizing this unique approach, viral vectors can be armed in such a way that transgene kinetics mimic the expression of the endogenous gene even if the exact transcriptional map of the vector is not fully defined.

The findings presented here demonstrate that the MAV-1 vector system is a suitable murine homolog system that can be used to model the mechanism of action of oncolytic adenoviral vectors in an immunocompetent, tumor-bearing host. Such a model potentially allows detailed evaluation of the effects of virus replication, immunomodulatory transgene expression, and the immune system on overall virus potency and provides a more complete assessment of vector safety, thus providing the translational data crucial for effectively moving these viruses into clinical development.

MATERIALS AND METHODS

Cells and viruses. All of the murine tumor cell lines used in this study were obtained from the American Type Culture Collection (ATCC) and maintained in full growth medium (FGM) Dulbecco modified Eagle medium (DMEM) High (SAFC Biosciences, Lenexa, KS) supplemented with 10% (vol/vol) fetal bovine serum and 1% (vol/vol) penicillin-streptomycin (Invitrogen, Carlsbad, CA). The Swiss albino fibroblast cell line 3T6-KS and the 37.1 cells used were described previously (58) 37.1 cells used were maintained in FGM DMEM High (SAFC Biosciences, Lenexa, KS) supplemented with 5% (vol/vol) fetal bovine serum, 1% (vol/vol) penicillin-streptomycin, and 200 μg/ml G418 (Invitrogen, Carlsbad, CA) as previously described (58). The murine cell lines used included the murine pancreatic carcinoma cell line Pan02 (National Cancer Institute DCTDC Tumor Repository, Frederick, MD), the murine bladder carcinoma cell line MB49 (obtained from T. Ratliff, University of Iowa), the murine colorectal carcinoma cell line CT26 (ATCC Cl-2638), the murine metastatic breast cancer cell line 4T1 (ATCC CL-2539), the murine fibrosarcoma cell line SAI (ATCC CL-2539), and primary murine embryonic fibroblasts (MEFs) (SJL; ArtisOptimus, Carlsbad, CA).

The previously generated mouse adenovirus vectors pmE301 (wild type) and *dl*E102 (containing an E1A CR2 deletion) were described previously (58, 67).

Construction of armed MAV-1 vectors. A large plasmid, pFL-dlE102, containing the full-length *dl*E102 genome (30,944 nucleotides [nt]) was constructed to generate armed MAV-1 vectors. The left-hand region of *dl*E102 (nt 1 to 1379) was amplified by PCR with primers GAGCTCTAGGGATAACAGGGTAATC ATCATCAATAATATACAGTT and GCGGCCGCCAACCATCACAAAAC GTCCCTCT. The right-hand region of *dl*E102 (nt 29886 to 30944) was amplified by PCR with primers GCGGCCGCGGACGACTGCCAATGTTCC and CTC GAGTAGGGATAACAGGGTAATCATCATCAATCCTCTACAGTTAGCA AAAAATGGCGC. The left-hand SacI/NotI fragment and the right-hand NotI/XhoI fragment were then cloned into pBluescript II (Stratagene, La Jolla, CA) digested with SacI and XhoI. The combined flanking regions were then subcloned as a blunt-ended SacI/XhoI fragment into the blunt cloning site in the pLC-SmartAmp vector (Lucigen, Middleton, WI) to generate the pLC-MAV-FR plasmid. The NotI-digested pLC-MAV-FR plasmid was cotransformed with *dl*E102 viral DNA into *Escherichia coli* BJ5183 cells to generate a full-length clone (pFL-dlE102) by homologous recombination (12, 28). To insert the mGM-CSF–furin–2A transgene cassette linked to the MAV-1 L3 23K gene, a shuttle plasmid (pBS MAV Not-Apa) was generated by inserting a NotI/ApaI fragment of *dl*E102 that contains the L3 region (nt 16744 to 22945) into pBluscript II digested with the same enzymes. The mGM-CSF cDNA was amplified by PCR from plasmid pKCC-mGMCSF with primers ATGTGGCTGCAGAATTTACTTTTCC TGGG and TCATTTTTGGACTGGTTTTTTGCATTCAAA. The furin-2A sequence was amplified from plasmid pRRKR2ADC101 (16) with primers AGAAA AAGAAGGGAAGCCAGAC and TGGACCTGGGTTGCTCTCAACAT. Two transgene cassettes were generated by the PCR splice overlap extension method (63). In the first cassette (LFM), the furin-2A sequences was placed 5′ of the mGM-CSF cDNA. This furin–2A–mGM-CSF sequence was then inserted 3′ of the MAV-1 L3 23K gene that had its stop codon removed. For the second cassette (MFL), the furin-2A sequence was placed 3′ of the mGM-CSF cDNA that had its stop codon removed and then this sequence was inserted 5′ of the MAV-1 L3 23K gene. These two cassettes were then cloned as SbfI/BamHI fragments into pBS MAV Not-Apa cut with the same enzymes. NotI/KpnI fragments were cotransformed with the SbfI-linearized pFL-dlE102 plasmid into *E. coli* BJ5183 cells to generate full-length clones. The full-length clones were then linearized by I-SceI digestion and transfected into 37.1 cells with Fugene 6 (Roche Diagnostics, Basel, Switzerland) to produce infectious virus.

Virus production. MAV-1 vectors were propagated in 37.1 cells as previously described (58). Twenty-four hours prior to infection, 37.1 cells were incubated in FGM with 1% (vol/vol) fetal bovine serum–1% (vol/vol) penicillin-streptomycin (Invitrogen, Carlsbad, CA) and supplemented with 1 μM dexamethasone to induce E1A expression. 37.1 cells were then infected with the vector at a multiplicity of infection (MOI) of 1 to 5. The infected cells were then incubated in DMEM High (SAFC Biosciences, Lenexa, KS) supplemented with 1% (vol/vol) fetal bovine serum, 1% (vol/vol) penicillin-streptomycin (Invitrogen, Carlsbad, CA), and 1 μM dexamethasone. Supernatants were harvested at 2 to 3 days postinfection. The virus stocks were assayed for virus titer (PFU per milliliter) on 37.1 cells as previously described (9). High-titer virus stocks were produced in cell factories (CF10; Fisher). CF10 cell factories were seeded with 37.1 cells in FGM DMEM supplemented with 5% (vol/vol) fetal bovine serum, 1% (vol/vol) penicillin-streptomycin, and 1 μM dexamethasone. When the cells reached 70 to 80% confluence, the medium was removed and replaced with FGM DMEM supplemented with 1% (vol/vol) fetal bovine serum, 1% (vol/vol) penicillin-streptomycin, and 1 μM dexamethasone. The cells were infected with the vector at an MOI of 5 to 10. The infected cells were incubated for 3 to 4 days at 37°C in 5% CO_2 until a complete cytopathic effect was observed. The supernatant was harvested from the CF10 and treated with 50 U/ml Benzonase (EMD Biosciences), and the cellular debris was pelleted by centrifugation at 2,000 rpm for 10 min. The supernatant was then clarified by filtration through a 0.45 ± 0.2-μm filter (Sartobran P; Sartorius AG, Germany) and concentrated by tangential-flow filtration through columns with a 750-kDa molecular mass cutoff (GE Healthcare). The concentrated supernatant underwent a buffer exchange process into a final formulation of phosphate-buffered saline (PBS) with 10% (vol/vol) glycerol. The purified virus was then aliquoted and stored at −80°C.

Virus production assays. Virus production assays were performed based on a method previously described (58). Briefly, cells were seeded at 24 h prior to infection and treated with 1 μM dexamethasone. The cells were then infected with virus at 5 PFU per cell in serum-free medium. After 90 min, the medium was removed and replaced with fresh FGM–1% (vol/vol) fetal bovine serum (FBS) and the supernatants were harvested at various time points after infection. The

levels of virus in supernatant samples were quantified with a 50% tissue culture infective dose ($TCID_{50}$) assay on 37.1 cells in a 96-well plate format and incubated for 8 days.

Cytotoxicity assays ($TCID_{50}$ assays). A 1-in-5 serial dilution of virus was used to infect a panel of murine tumor and nontumor cell lines in a 96-well plate format. The cells were incubated for 8 days in FGM–1% FBS, their viability was assessed by the addition of 3-(4,5-dimethylthiazol-2-yl)-5-(3-carboxymethoxyphenyl)-2-(4-sulfophenyl)-2*H*-tetrazolium reagent (MTS; CellTiter 96 AQueous One Solution cell proliferation assay; Promega, Madison, WI), and their optical density at 450 nm was determined (Spectramax spectrophotometer; Molecular Devices, Sunnyvale, CA). Data were analyzed with the Prism 4 software (GraphPad, San Diego, CA).

GM-CSF expression assays. For the in vitro assays, 37.1 cells were seeded 24 h prior to infection and treated with 1 μM dexamethasone. The cells were infected with virus at 5 PFU per cell in serum-free medium. After 90 min, the medium was removed and replaced with fresh FGM–1% FBS–1 μM dexamethasone with or without 20 μg/ml cytosine-β-D-arabinofuranoside (AraC; Sigma, St. Louis, MO) and the supernatant was sampled at various time points. The human GM-CSF level in the supernatants was quantified by enzyme-linked immunosorbent assay (ELISA; R&D Systems, Minneapolis, MN).

In vivo efficacy assays. Mice (4 to 6 weeks of age; body weight of 18 to 20 g) were purchased from Simonsen Laboratories (Gilroy, CA). Mice were housed in accordance with AAALAC guidelines. Study designs were approved and performed according to the guidelines of the Cell Genesys Animal Use and Care Committee. Female BALB/c or C57BL/6 mice were injected subcutaneously in the right flank with either 5×10^5 CT26 cells (injection volume of 500 μl) or 2.5×10^6 Pan02 cells (injection volume of 200 μl), respectively. When tumors reached the desired mean volume (~150 mm^3 for CT26, 60 to 90 mm^3 for Pan02), as determined by the formula Volume (in cubic millimeters) = $W \times (L)^2/2$ (W, width; L, length), animals were randomly distributed into treatment groups. Mice received either virus or the vehicle via intratumoral (i.t.) injections under various dosing regimens. Tumor size was measured twice weekly in two dimensions. When tumor volumes reached 2,000 mm^3 or the tumors became necrotic, animals were euthanized. Effects of the vector treatment were monitored by weekly body weight measurements.

In vivo mGM-CSF expression and virus replication assay. Tumor-bearing mice were injected i.t. with 1×10^7 PFU in 50 μl of vector. Animals were subsequently euthanized at various time points, and the tumors were harvested. The tumors were homogenized, and the levels of mGM-CSF were determined by ELISA (R&D Systems, Minneapolis, MN). The values were normalized to the total protein concentration of the homogenate as determined by the BCA Protein Assay (Pierce, Rockford, IL). To determine virus genome copy numbers, DNA was extracted from the homogenates with the Qiagen Tissue DNA Extraction kit (Qiagen, Valencia, CA). The number of adenovirus genome copies present in the sample was then determined with quantitative PCR (qPCR) primer sets specific for MAV-1 (40) or Ad5 (51) as previously described. The values were normalized to the level of murine genomic DNA present, as indicated by the level of murine ApoB DNA determined by qPCR with forward (CGTGGGCTCCAGCATTCTA) and reverse (AGTCATTTCTGCCTTTGC GTC) primers specific for ApoB in combination with an ApoB-specific probe (6-carboxyfluorescein–CCAATGGTCGGGCACTGCTCAA–6-carboxytetramethylrhodamine).

Immune cell characterization and flow cytometry. Cells from spleens were collected and mechanically dissociated with glass slides either 10 days after tumor rechallenge (CT26 model) or 10 days after the last virus administration (Pan02 model). Cells were counted and stained with conjugated antibodies in accordance with the manufacturer's protocol (BD Pharmingen, San Diego, CA). Flow cytometry acquisition and analysis were performed with the FACScan apparatus and CellQuest Pro software (BD Biosciences, San Diego, CA). Splenocytes were coincubated with irradiated tumor cells (ratio of 50 effector cells to 1 target cell), and antigen-specific responses were determined by a gamma interferon (IFN-γ) enzyme-linked immunospot assay (R&D Systems, Minneapolis, MN) as previously described (42). Levels of cytokine secretion by antigen-stimulated splenocytes were determined in supernatants at 48 h poststimulation by Cytokine Bead Array (BD Pharmingen, San Diego, CA).

Statistical analysis. Statistical analysis of tumor progression between different groups was performed by linear regression based on the best fit of the linear portion of the curve and statistical analysis to determine if the slopes were different. Multiparameter statistics for Kaplan-Meier survival curves were performed with a log rank test. Relative differences between groups were analyzed by a one-way analysis of variance (ANOVA) with a Bonferroni correction. All statistical analyses were performed with GraphPad Prism (GraphPad Software, La Jolla, CA).

RESULTS

In vitro evaluation of *dl*E102 as an oncolytic virus. For *dl*E102 to serve as a murine oncolytic vector homolog for human conditionally replication-competent adenovirus vectors, the murine vector must be able to replicate in and kill a wide variety of murine tumor cells while demonstrating attenuated replication in nontransformed murine cells compared to that of the unmodified wild-type vector. The cytotoxicity of *dl*E102 was evaluated in various murine tumor cell lines in vitro and compared to that of the wild-type MAV-1 vector, pmE301 (67) (Fig. 1A). Half-maximal effective concentrations (EC_{50}s) were measured in the Pan02 (pancreatic), CT26 (colon), MB49 (bladder), 4T1 (breast), SAI (sarcoma), and CMT64 (lung) murine tumor cell lines at 8 days postinfection to allow direct comparison of EC_{50}s across the various cell lines. In all of these tumor cell lines, the wild-type pmE301 and *dl*E102 vectors had comparable EC_{50}s, ranging from 0.01 to 10 PFU ml^{-1}, which is comparable to the range seen with human oncolytic adenoviruses in human tumor cells (0.013 PFU ml^{-1} in highly permissive Hep3B cells [7] to 17.0 PFU ml^{-1} in less permissive RPMI2650 cells [50]). Both *dl*E102 and wild-type MAV-1 had 2- to 3-log lower average EC_{50}s than the human Ad5-E2F virus (range, 5 to 500 PFU ml^{-1}), demonstrating the superior cytotoxicity of MAV-1 vectors in murine cells.

The cytotoxicity of *dl*E102 (Fig. 1B and C) was compared to that of wild-type pmE301 in Pan02 tumor cells and SJL MEFs to determine if virus replication was attenuated in nontransformed cells. Wild-type pmE301 and the oncolytic *dl*E102 vectors had comparable EC_{50}s in the Pan02 tumor cell line (0.72 and 0.92 PFU ml^{-1}, respectively), whereas the EC_{50} of the oncolytic *dl*E102 vector (0.38 PFU ml^{-1}) was 20-fold lower (0.02 PFU ml^{-1}) than that of the wild-type pmE301 vector in nontransformed murine fibroblasts, comparable to the 20-fold attenuation of a human oncolytic Ad5-based vector compared to wild-type Ad5 in nontransformed human WI-38 fibroblast cells (50). These data showed that the MAV-1 vectors are highly effective at killing murine tumor cells and that the murine *dl*E102 vector has attenuated replication and reduced cytotoxicity in nontransformed fibroblast cells compared to wild-type pmE301. It should be noted that while nontransformed fibroblasts were used in this assay, Pan02 cells are of epithelial origin. As stated previously, epithelial cells are host cells for MAV-1 and further studies on the growth of the MAV-1 vectors in nontransformed epithelial cells are therefore needed to determine if the cell type used has an effect on virus cytotoxicity.

In vivo evaluation of *dl*E102 as an oncolytic virus. The ability of *dl*E102 to control the growth of established tumors in immunocompetent mice in vivo was evaluated. Immunocompetent mice bearing subcutaneous (s.c.) CT26 colon carcinomas ($n = 10$ per group) were injected i.t. three times (at days 8, 11, and 15 after tumor inoculation) with the vehicle (PBS–10% glycerol), the *dl*E102 vector (1×10^7 PFU per injection), or the heat-inactivated *dl*E102 vector (50 μg of protein per injection) (Fig. 2A). In the vehicle and heat-inactivated *dl*E102 groups, tumors increased in size until they reached a maximum volume of 2,000 mm^3 and the animals were euthanized, giving a median survival time (MST) of 28 days post tumor inoculation (dpi) (data not shown). In contrast, tumor growth was signifi-

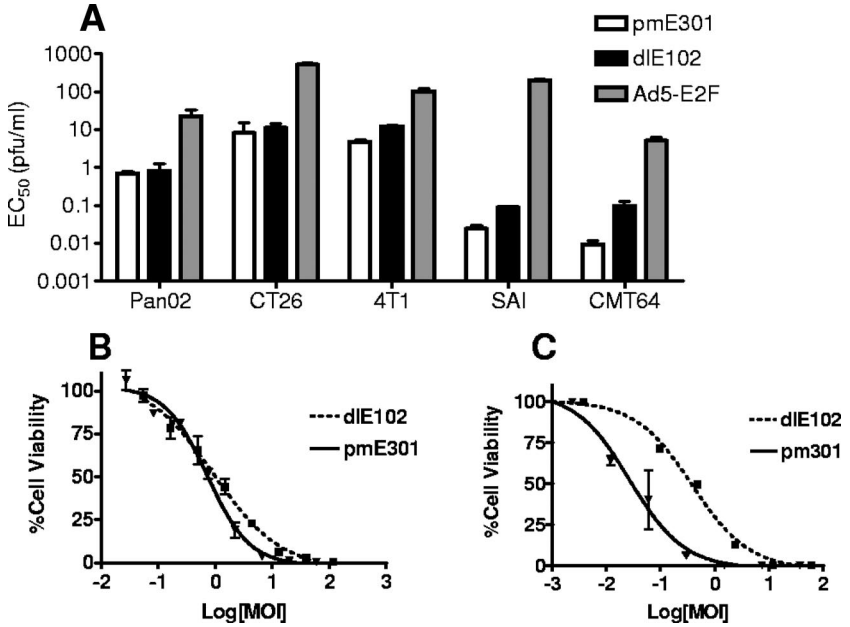

FIG. 1. In vitro oncolytic properties of the *dl*E102 MAV-1 vector. (A) The EC_{50}s were determined for the pmE301 (wild-type MAV-1), *dl*E102 (MAV-1 containing a CR2 deletion), and Ad5-E2F vectors in a panel of murine tumor cell lines, including pancreatic cancer (Pan02), colon cancer (CT26), breast cancer (4T1), sarcoma (SAI), and small-cell lung cancer (CMT64) cell lines. Cells were infected in triplicate with a 1-to-5 serial dilution of vector starting at 10,000 PFU/cell in DMEM–1% FBS. Cell viability was assessed after 8 days with a tetrazolium salt-based assay (MTS reagent). The EC_{50}s were determined with the GraphPad Prism software. Killing curves were obtained for pmE301 and *dl*E102 in (B) murine pancreatic tumor cells (Pan02) and (C) normal murine fibroblasts (SJL MEFs). Cells were infected in triplicate with a 1-to-5 serial dilution of vector starting at 10,000 PFU/cell in DMEM–1% FBS. Cell viability was assessed at 8 days postinfection with a tetrazolium salt-based assay (MTS reagent).

cantly delayed in animals injected with live *dl*E102 virus, with an average tumor volume of ~900 mm^3 by 30 dpi, resulting in an improved MST of 42 dpi (data not shown).

To determine whether the observed antitumor activity of *dl*E102 was due to virus replication, mice bearing CT26 tumors ($n = 5$ per group) were injected with a single dose (1×10^7 PFU) of *dl*E102 or Ad5-E2F at 8 dpi, when tumors had reached an average volume of 150 mm^3. Tumors were harvested 3, 5, and 7 days after virus injection, and the level of virus genomes was determined by qPCR of genomic DNA extracted from tumors, normalized to tumor size by the comparative level of murine ApoB copies (Fig. 2B). In *dl*E102-injected tumors, an approximately 2-log increase in virus genome copy numbers was observed from day 3 to day 5, suggesting that the virus was replicating. The level of *dl*E102 genomes decreased by day 7 postinjection, potentially due to the clearance of virus-transduced cells by the immune system. In contrast, the highest level of viral genomes for Ad5-E2F was observed 3 days after virus injection and the number of genomes decreased rapidly with time, suggesting a lack of i.t. virus replication that correlated with poor antitumor activity. An initial higher level of Ad5 genomes than *dl*E102 genomes was detected at 3 dpi, even though comparable doses were administered (1×10^7 PFU, as determined by plaque assay). This difference could be due to several factors, including differences in sensitivity between the Ad5 and MAV-1 plaque assays, differences in the PFU/viral particle ratio, or differences in the rate of cellular uptake and/or initial clearance of the vector from within the tumor. To further evaluate these differences, earlier time points after initial administration need to be assessed. These findings suggest that the antitumor activity of *dl*E102 in CT26 tumor-bearing immunocompetent mice is due to the cytotoxicity of the vector caused by i.t. virus replication.

Since tumors started progressing after virus injections stopped, a follow-up study was conducted to determine whether tumor growth could be controlled for a longer period of time with repeat administrations of *dl*E102. Mice bearing CT26 tumors ($n = 10$ per group) were injected i.t. either once or twice weekly (1×10^7 PFU per dose) with *dl*E102. Tumor progression and the overall survival of these animals were compared to those of tumor-bearing mice injected twice weekly with the vehicle (Fig. 2C). At 22 dpi, mice treated with a weekly dose of *dl*E102 showed a delay in tumor progression (average tumor volume of 600 mm^3) compared to that of the vehicle-injected control group (average tumor volume of 950 mm^3). An even greater delay in tumor progression was observed in the group injected twice weekly with the *dl*E102 vector (average tumor volume of 370 mm^3). Mice injected with the vehicle had an MST of 27 days, with 1/10 mice tumor free at day 70, whereas the group injected with a weekly dose of *dl*E102 demonstrated an increase in MST to 39 days ($P < 0.31$), with 2/10 mice tumor free at day 70 (Fig. 2D). In the twice-weekly treatment group, the MST was increased to >70 days and the overall survival was significantly increased (6/10 surviving at day 70; $P < 0.005$). These data demonstrated the potent antitumor activity of *dl*E102 in the s.c. CT26 tumor model and suggested that repeated virus injections translate

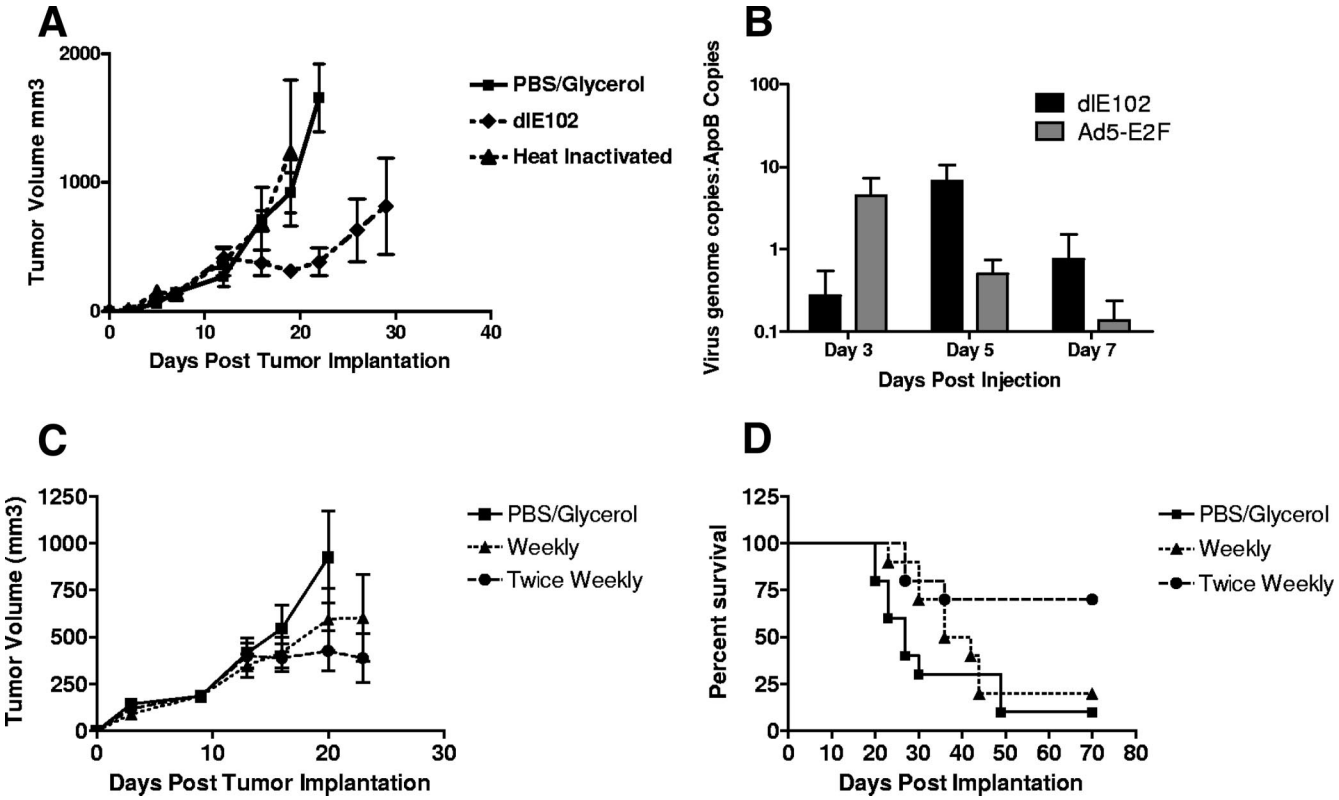

FIG. 2. In vivo efficacy of *dl*E102 in an immunocompetent syngeneic tumor model. (A) Female BALB/c mice bearing subcutaneous CT26 tumors were injected i.t. when the average tumor size reached approximately 150 mm^3 with the vehicle (PBS–10% [vol/vol] glycerol), *dl*E102 (1×10^7 PFU in a 50-μl volume), or heat-inactivated *dl*E102 (50 μg of total protein in a 50-μl volume) on days 8, 10, and 15 post tumor implantation for a total of three injections. Tumor volume was determined by caliper measurement and expressed as the mean tumor volume (cubic millimeters plus the standard error of the mean; $n = 5$ per group). (B) The level of virus replication within the tumor was determined in female BALB/c mice bearing CT26 tumors with a single i.t. injection of 1×10^7 PFU *dl*E102 or Ad5-E2F. Mice were euthanized 3, 5, and 7 days post virus injection, tumors were homogenized, the genomic and viral DNAs were extracted, and the number of adenovirus genome copies in the liver was determined by qPCR. The data are presented as the number of virus genome copies per copy of cellular ApoB genome to normalize for total genomic DNA content. (C and D) The effect of repeat administration of the *dl*E102 vector was determined in the CT26 tumor model. Female BALB/c mice bearing subcutaneous CT26 tumors were injected i.t. with the vehicle (PBS–10% [vol/vol] glycerol) twice weekly or either a weekly dose or a twice-weekly dose of *dl*E102 (1×10^7 PFU in a 50-μl total volume). The tumor volume (panel C; cubic millimeters plus the standard error of the mean; $n = 10$ per group) and overall survival (panel D) were determined.

into better overall survival of tumor-bearing animals with no apparent toxicity.

Arming the *dl*E102 vector with murine GM-CSF by using the foot and mouth disease virus (FMDV) 2A sequence. At least one oncolytic adenoviral vector currently being evaluated in clinic (CG0070) has been armed with the immunomodulatory cytokine GM-CSF (7, 49). The aim of using these armed vectors is to enhance potency by inducing a systemic, tumor-specific immune response via the expression of GM-CSF at the site of virus-mediated tumor cell killing. GM-CSF is known to recruit dendritic cells, which subsequently take up and present antigens to T cells in a process called cross-presentation. It is thus possible that locally administered viruses could potentially treat metastatic disease, serving, in effect, as an in situ immunotherapy. A novel approach that linked mGM-CSF transgene expression to MAV-1 L3 23K protease gene expression via FMDV-derived 2A and furin protease cleavage sequences was used to arm *dl*E102 with mGM-CSF. This approach has previously been shown to allow equimolar expression of two genes linked by the 2A-furin sequences and expressed from a single promoter (16). During the protein translation process, the 2A peptide self-cleaves, leading to initial cleavage of the two proteins, and the furin cleavage sequence enables endogenous furin cleavage of residual amino acids derived from the 2A cleavage sequence from the C terminus of the first protein located downstream of the promoter. Armed *dl*E102 vectors were constructed by inserting the 2A-furin transgene expression cassette either upstream (DMFL) or downstream (DLFM) of the MAV-1 L3 gene; this gene is homologous to the human Ad5 23K protease gene that is reported to be a suitable insertion site for achieving a high level of transgene expression when transgenes are linked to viral genes by a splice acceptor sequence (51) (Fig. 3). To determine the effect of the transgene insertion site on virus growth, cytotoxicity, and transgene expression levels, cells were infected in vitro with mGM-CSF-armed virus (MOI = 5) and the amount of virus in the supernatant was determined at various time points postinfection with a $TCID_{50}$ assay (Fig. 4A). Virus growth was evaluated in 3T6 cells (Fig. 4A), which is a natural producer cell line for MAV-1 (2), and in the murine pancreatic carcinoma cell line

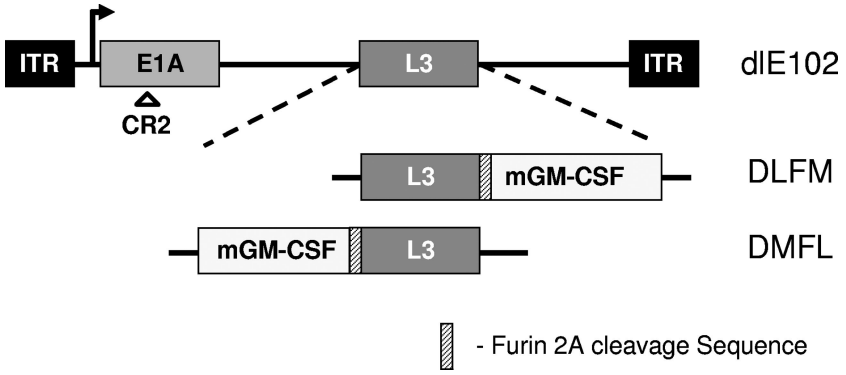

FIG. 3. Arming of the *dl*E102 vector with mGM-CSF by using the furin-2A cleavage sites. mGM-CSF-armed vectors were generated from the parental *dl*E102 vector that contained a deletion in the high-affinity *pRB* binding domain (CR2). In the DLFM vector, the furin–2A–mGM-CSF cassette was placed after the last codon of the MAV-1 L3 gene and the L3 stop codon was removed. In the DMFL vector, the mGM-CSF–furin–2A cassette was placed immediately upstream of the MAV-1 L3 gene. ITR, inverted terminal repeat.

Pan02 (Fig. 4B). Comparable levels of the parental *dl*E102 virus and the DLFM virus were found in the supernatant of transduced cells, with maximum virus yields obtained between 48 and 72 h postinfection in both the 3T6 and Pan02 cell lines (~10,000 PFU ml^{-1} and ~20,000 PFU ml^{-1}, respectively). The DMFL vector produced, on average, three- to fourfold less virus in both cell lines (~3,000 and ~5,000 PFU ml^{-1}, respectively) than did *dl*E102 or DLFM. The EC_{50}s were generated for the parental *dl*E102, DLFM, and DMFL vectors in 3T6 and Pan02 cells as described earlier in order to determine whether the transgene insertion site affected the overall cytotoxicity of the armed viruses (Fig. 4C). As with the comparative virus yield, *dl*E102 and DLFM had similar EC_{50}s in 3T6 (0.67 and 0.66 PFU ml^{-1}, respectively) and Pan02 (0.06 and 0.03 PFU ml^{-1}, respectively) cells, whereas a threefold higher EC_{50} was observed for the DMFL vector in both cell lines (1.886 and 0.165 PFU ml^{-1}, respectively).

Transgene expression in the supernatants of 3T6 and Pan02 virus-infected cells was determined by measuring mGM-CSF levels at 72 h postinfection (Fig. 5A). The DLFM vector produced the highest levels of mGM-CSF (321,030 pg/ml in 3T6 cells and 500,871 pg/ml in Pan02 cells). Comparatively, DMFL vector-infected 3T6 and Pan02 cells secreted 2- to 20-fold lower mGM-CSF levels (19,910 and 259,670 pg/ml, respectively). Thus, while the insertion of the transgene expression cassette upstream of the MAV1 L3 gene (DMFL) had a deleterious effect on virus growth and cytotoxicity, resulting in lower overall transgene expression, insertion downstream of

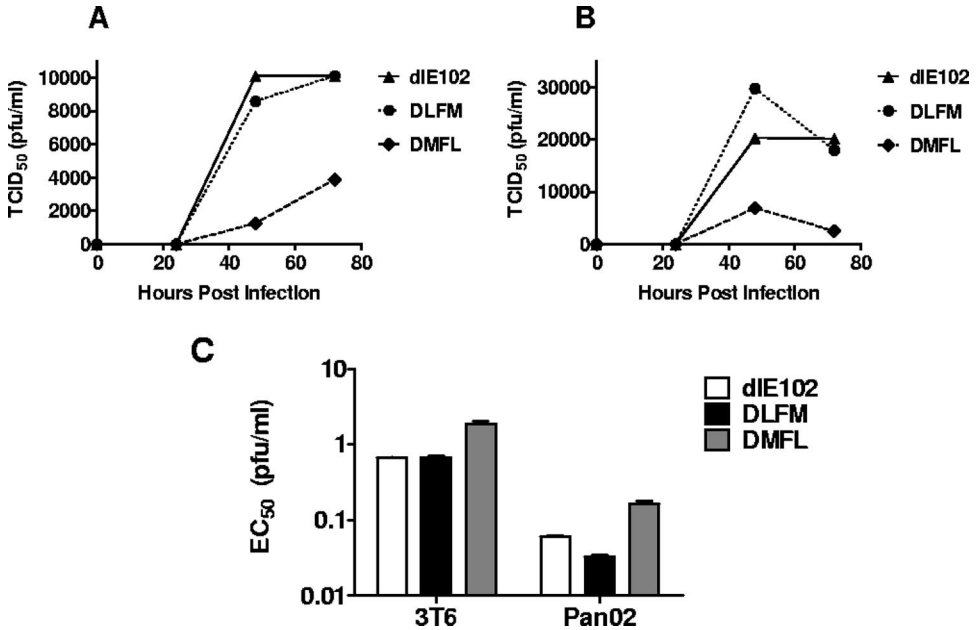

FIG. 4. Effect of transgene insertion on virus growth and cytotoxicity of armed MAV-1 vectors. 3T6 murine fibroblasts (A) and Pan02 murine tumor cells (B) were infected with *dl*E102, DLFM, or DMFL at an MOI of 5 PFU/cell in duplicate, and the supernatants were collected at 24, 48, and 72 h postinfection. Viral yield was determined by a $TCID_{50}$ assay, and the data were plotted as the $TCID_{50}$ (PFU per milliliter) versus time. (C) EC_{50}s were generated on both 3T6 and Pan02 cells as described in the legend to Fig. 1.

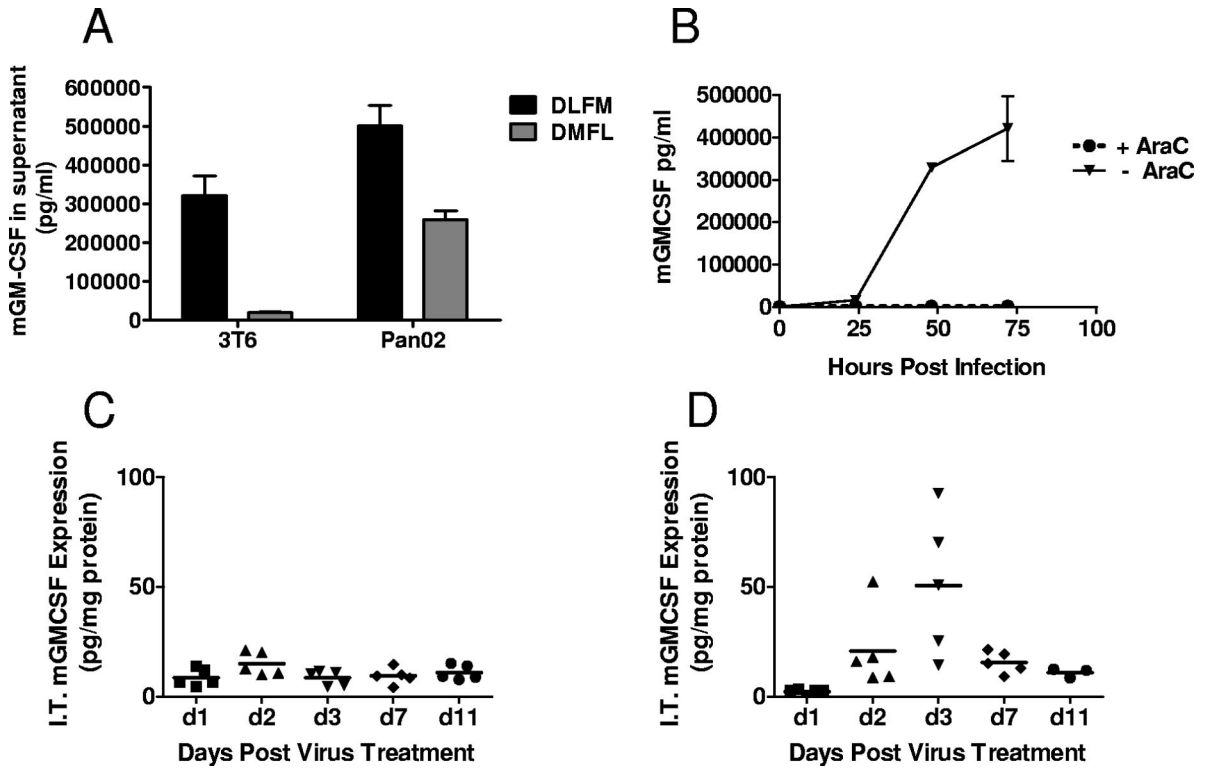

FIG. 5. In vitro and in vivo transgene expression from armed MAV-1. For in vitro transgene expression (A), 3T6 and Pan02 cells were infected with DLFM or DMFL at an MOI of 5 PFU/cell in duplicate, the supernatants were collected at 72 h postinfection, and GM-CSF levels (mean ± the standard error of the mean) were determined by ELISA. (B) For the DLFM vector, infection of Pan02 cells was performed in the presence (dotted line) or absence (solid line) of 20 μg/ml AraC, a DNA replication inhibitor, to determine if transgene expression occurred in the absence of viral DNA replication. For in vivo transgene expression, female C57BL/6 mice bearing subcutaneous Pan02 tumors ($n = 5$ per group) were injected i.t. with a single dose (1×10^7 PFU in a 50-μl volume) of *dl*E102 (C) or DLFM (D). The tumors were harvested at 1, 2, 3, 7, and 11 days posttreatment, and the i.t. level of mGM-CSF was determined by ELISA and normalized to tumor size by determining the total protein content of the tumor homogenate. The data are presented as milligrams of mGM-CSF per milligram of total protein for individual animals at the various time points.

the MAV-1 L3 gene (DLFM) had no impact on these virus properties.

When virus replication was blocked in Pan02 cells by AraC (26) (Fig. 5B), no transgene expression from the DLFM vector was observed, suggesting that transgene expression from the MAV-1 L3 region is dependent on virus replication. Transgene expression was also determined in vivo after a single i.t. injection (1×10^7 PFU) of *dl*E102 or DLFM virus into immunocompetent animals bearing Pan02 tumors with an average tumor volume of 100 mm^3 (Fig. 5C and D). A peak i.t. mGM-CSF level of 50.7 pg/mg of total protein was observed at 3 days post DLFM virus injection and decreased over time to 10.9 pg mGM-CSF per mg of total protein by day 11 (Fig. 5D). The timing of the GM-CSF peak in the tumor post DLFM virus injection and the peak of *dl*E102 virus replication both occurred at 3 days postinjection. No i.t. mGM-CSF was observed in tumors injected with the parental *dl*E102 vector (Fig. 5C), indicating that the mGM-CSF in the DLFM-transduced tumors was generated by the injected virus and not secreted by immune cells that infiltrated the tumors after virus injection. These studies demonstrate for the first time that the 2A-furin cleavage site can be used to successfully arm viral vectors with a transgene by linking transgene expression to virus replication, resulting in high-level transgene expression without impacting the life cycle of the virus.

GM-CSF-armed MAV-1 vectors demonstrate antitumor activity in vivo. The in vivo antitumor activity of the mGM-CSF-armed DLFM vector was determined in immunocompetent BALB/c mice bearing s.c. CT26 colon carcinomas (Fig. 6). Tumor-bearing mice ($n = 10$ per group) were injected twice weekly with the vehicle (PBS–10% glycerol, 50-μl volume), *dl*E102, or DLFM (each at 1×10^7 PFU per dose, 50-μl volume). Tumor progression (Fig. 6A) and survival (Fig. 6B) were determined. In vehicle-injected mice, the tumors progressed rapidly, reaching an average volume of 750 mm^3 by 20 days postinjection, resulting in an MST of 34.5 days. In this group, 3/10 mice were tumor free due to spontaneous tumor regression, an observation previously described for this immunogenic tumor model (41). A significant delay in tumor progression (determined by linear regression analysis) was observed in the groups injected with either the *dl*E102 or the DLFM vector compared to vehicle-injected mice ($P < 0.0001$ and $P < 0.0008$, respectively), resulting in 9/10 and 8/10 mice being tumor free at day 70. An MST was not reached in either group. No significant difference in tumor progression ($P < 0.13$) or overall survival ($P < 0.57$) was seen between tumor-bearing

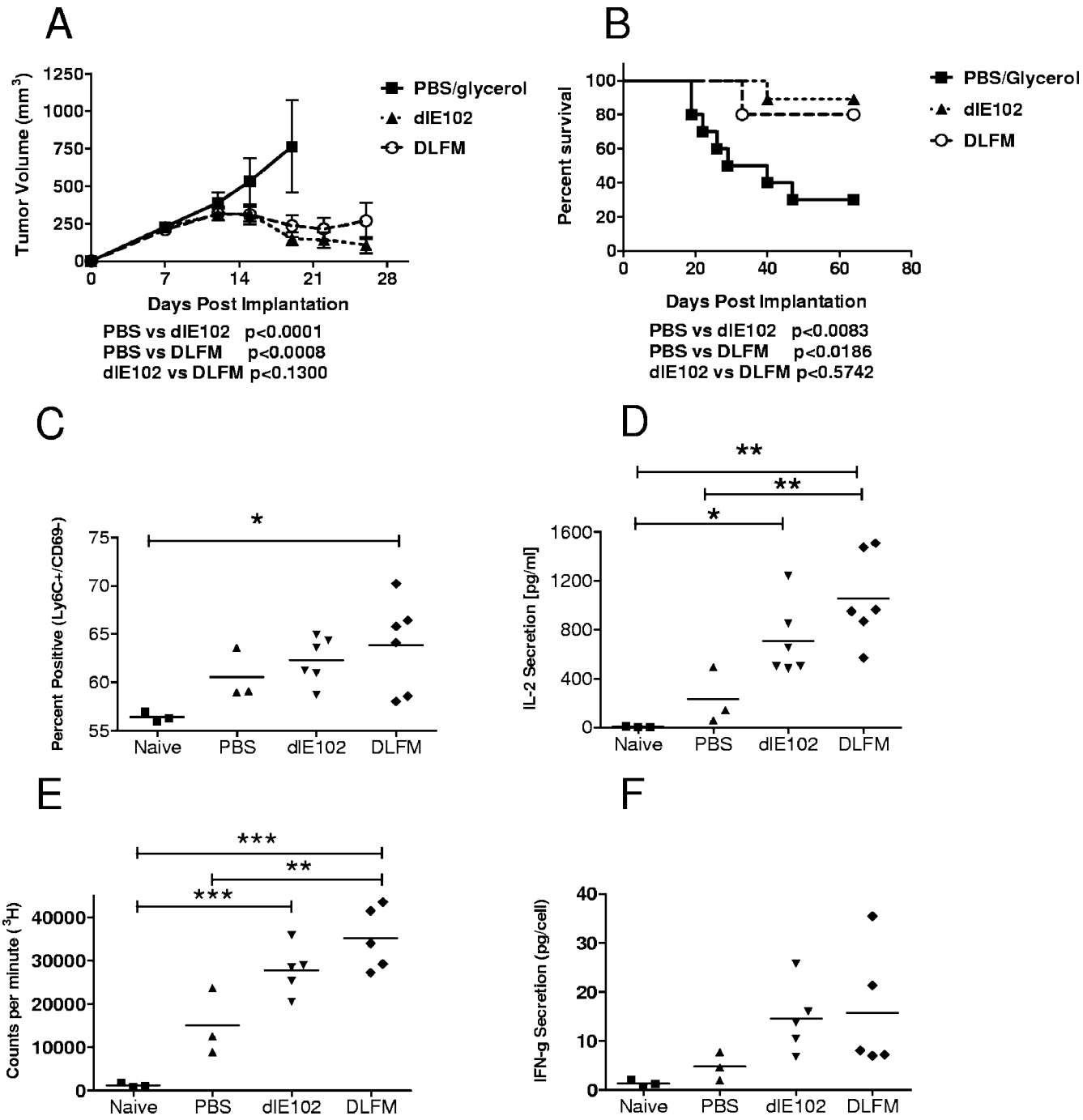

FIG. 6. Antitumor activity of armed MAV-1 vectors in the highly immunogenic CT26 xenograft tumor model. The DLFM vector was injected into CT26 s.c. tumor-bearing animals, and tumor progression (A) and overall survival (B) were determined. Female BALB/c mice bearing s.c. CT26 tumors (~150 mm^3) were injected twice weekly i.t. with the vehicle (PBS–10% [vol/vol] glycerol), *dl*E102, or DLFM (1×10^7 PFU in a 50-μl volume). Tumor volume (A) was determined by caliper measurement and expressed as the mean tumor volume (cubic millimeters plus the standard error of the mean, $n = 10$ per group). Mice whose tumors had been completely eradicated after injection with PBS ($n = 3$), *dl*E102, or DLFM (in both groups, $n = 6$) were rechallenged with CT26 cells. In addition, a naïve control group ($n = 3$) was also challenged with CT26 cells. Spleens were harvested at 10 days postchallenge, and the percentage of positive $CD8^+$ memory T cells (C) was determined by direct antibody staining and FACS analysis. Spleens were stimulated by coincubation with irradiated CT26 cells, and the levels of IL-2 secretion (D), cell proliferation (E), and antigen-specific IFN-γ secretion (F) were determined. Differences between groups were analyzed by a one-way ANOVA with a Bonferroni correction (*, $P < 0.5$; **, $P < 0.01$; ***, $P < 0.001$); they were not significant for IFN-γ.

animals treated with the *dl*E102 or the DLFM vector, possibly due to the highly immunogenic nature of the CT26 tumor. Tumor cell death induced by even an unarmed oncolytic virus may be sufficient to induce a systemic tumor-specific immune response without the need for the additional adjuvant GM-CSF. In support of this hypothesis is the presence of a systemic anti-CT26 specific memory response in mice 56 days after *dl*E102 injection, which was potent enough to protect all of the

animals from a lethal challenge dose of live CT26 tumor cells (data not shown).

To further evaluate this finding, the host immune response after rechallenge with CT26 cells was analyzed (Fig. 6C to F) in surviving mice that had originally been injected with PBS ($n = 3$), *dl*E102, or DLFM ($n = 6$ per group) and compared to that of naive mice that had not previously been inoculated with CT26 cells ($n = 3$). Ten days after rechallenge, the mice were euthanized and the spleens were harvested. Splenocytes were phenotyped by direct antibody staining and fluorescence-activated cell sorter (FACS) analysis (Fig. 6C) to determine the population of memory T cells ($Ly6C^+/CD69^-$) (42). In the group that had previously been treated with the DLFM vector, a significantly higher percentage ($P < 0.05$) of memory T cells was found than in naïve animals. An increase in memory T cells was also observed in the DLFM group compared to both the PBS and *dl*E102 groups, but the increase was not statistically significant ($P > 0.05$, respectively). Splenocytes were further restimulated with irradiated CT26 cells to assess the presence of CT26-specific activated T cells by analyzing standard markers of immune activation, including interleukin-2 (IL-2) and IFN-γ, in the cell culture supernatant (secretion levels were normalized to the number of IFN-γ-secreting cells, as determined by enzyme-linked immunospot assay) and by measuring cell proliferation (Fig. 6D to F). A statistically significant increase in IL-2 secretion ($P < 0.01$) and better overall cell proliferation ($P < 0.001$) were observed in animals injected with *dl*E102 or DLFM compared to the naïve group. The levels of IL-2 secretion and cell proliferation were increased in the *dl*E102-injected group compared to those of the PBS-injected group, but this was not statistically significant. However, there was a significant increase ($P < 0.01$) in IL-2 secretion and cell proliferation in the groups injected with DLFM compared to the PBS-injected groups. In addition, IFN-γ secretion was increased in splenocytes from mice injected with *dl*E102 or DLFM compared to the PBS-injected or naive mice; this increase, however, was not statistically significant. Although all four measures of tumor-specific immune activation were increased in animals injected with DLFM compared to *dl*E102, none of the increases reached statistical significance. In summary, expression of mGM-CSF from a murine oncolytic adenovirus did not increase tumor-specific immune responses to a level that translated into prolongation of the survival of mice bearing highly immunogenic CT26 tumors compared to that of animals injected with an oncolytic adenovirus not expressing GM-CSF.

In a follow-up study, the ability of the adjuvant GM-CSF to increase the efficacy of oncolytic viruses was evaluated in the poorly immunogenic Pan02 pancreatic tumor model. This model is classified as poorly immunogenic, as no spontaneous regression occurs after a challenge of mice with live tumor cells and immunostimulatory agents such as IL-12 are unable to induce a tumor-specific immune response in animals with established tumors (38). C57BL/6 mice bearing Pan02 tumors (average volume of 70 to 80 mm^3) were injected weekly (a total of six injections) with 50 μl of either the vehicle (PBS–10% glycerol, $n = 10$) or 1×10^7 PFU of *dl*E102 ($n = 9$) or DLFM ($n = 7$), and tumor progression (Fig. 7A) and overall survival (Fig. 7B) were determined. In the PBS-injected group, tumors progressed steadily, reaching an average volume of 308 mm^3 by 54 dpi, resulting in an MST of 61 days. No delay in tumor progression (average volume of 312 mm^3 at day 54) or improvement in overall survival (MST = 64.5 days) was observed in the group injected with the *dl*E102 vector. In contrast, a statistically significant delay in tumor progression was observed in animals injected with the DLFM vector (average tumor volume of 193 mm^3 at 54 dpi) compared to either the PBS- or *dl*E102-injected group ($P < 0.001$ and $P < 0.014$, respectively). A significant prolongation of survival in the DLFM group was observed (MST = 75 dpi) compared to the PBS-injected group ($P < 0.0143$) but not the *dl*E102 group ($P < 0.3554$). These findings show that although the *dl*E102 vector had overall low antitumor activity in the poorly immunogenic Pan02 tumor model, treatment with the GM-CSF-armed DLFM virus did significantly decrease the tumor growth rate.

To evaluate the extent of immune activation in this model, mice bearing Pan02 tumors ($n = 6$ per group) received two injections, a week apart, of PBS (50 μl), *dl*E102, or DLFM (each at 1×10^7 PFU in 50 μl). Mice were euthanized 10 days later, and splenocytes were analyzed by costaining $CD4^+$ and $CD8^+$ T cells for the T-cell activation markers CD44 and CD62L, followed by FACS analysis (43) (Fig. 7C and D). In the DLFM-injected group, a significantly higher percentage of activated T cells ($CD44^{hi}/CD62L^{lo}$) was detected in the $CD4^+$ T-cell population. ($P < 0.05$). A higher percentage of activated $CD8^+$ T cells ($P < 0.05$) was also observed in the DFLM-injected group than in the *dl*E102-injected group, but this was not significant, demonstrating that i.t. expression of GM-CSF from an oncolytic adenovirus can significantly increase the activation of a systemic antitumor immune response. Further, this activation is potent enough to control the tumor growth rate, especially in mice bearing poorly immunogenic tumors.

DISCUSSION

An in vivo tumor model is required that can accurately model the effects of both virus replication and the immune system on tumor growth to fully evaluate the efficacy and safety of oncolytic adenoviral vectors. The inability of human adenovirus to replicate efficiently in murine cells has, to date, limited the preclinical evaluation of armed oncolytic adenoviruses. Alternate animal models such as the cotton rat (61) and the Syrian hamster (60) have previously been described for this purpose, but their use has been limited by the lack of syngeneic tumor cell lines, species-specific transgenes, and suitable reagents to permit monitoring of immune responses.

In this study the feasibility of using a species-specific MAV-1 vector, *dl*E102, as an oncolytic vector in an immunocompetent syngeneic tumor model was examined. *dl*E102 has a deletion in the high-affinity pRb-binding domain (CR2). Deletion of the CR2 region in human Ad5-based vectors has previously been shown to restrict the replication of these vectors to tumor cells that are defective in the pRb pathway (21). In this study, the *dl*E102 virus was shown to be more cytotoxic in a wide range of murine tumor cells in vitro than an Ad5-based vector. *dl*E102 had cytotoxicity comparable to that of the wild-type pmE301 vector in tumor cells but was 20-fold less cytotoxic in untransformed murine fibroblasts, demonstrating that its tumor selectivity is similar to that of the human Ad5-based oncolytic vectors currently being developed in clinic. *dl*E102 also replicates

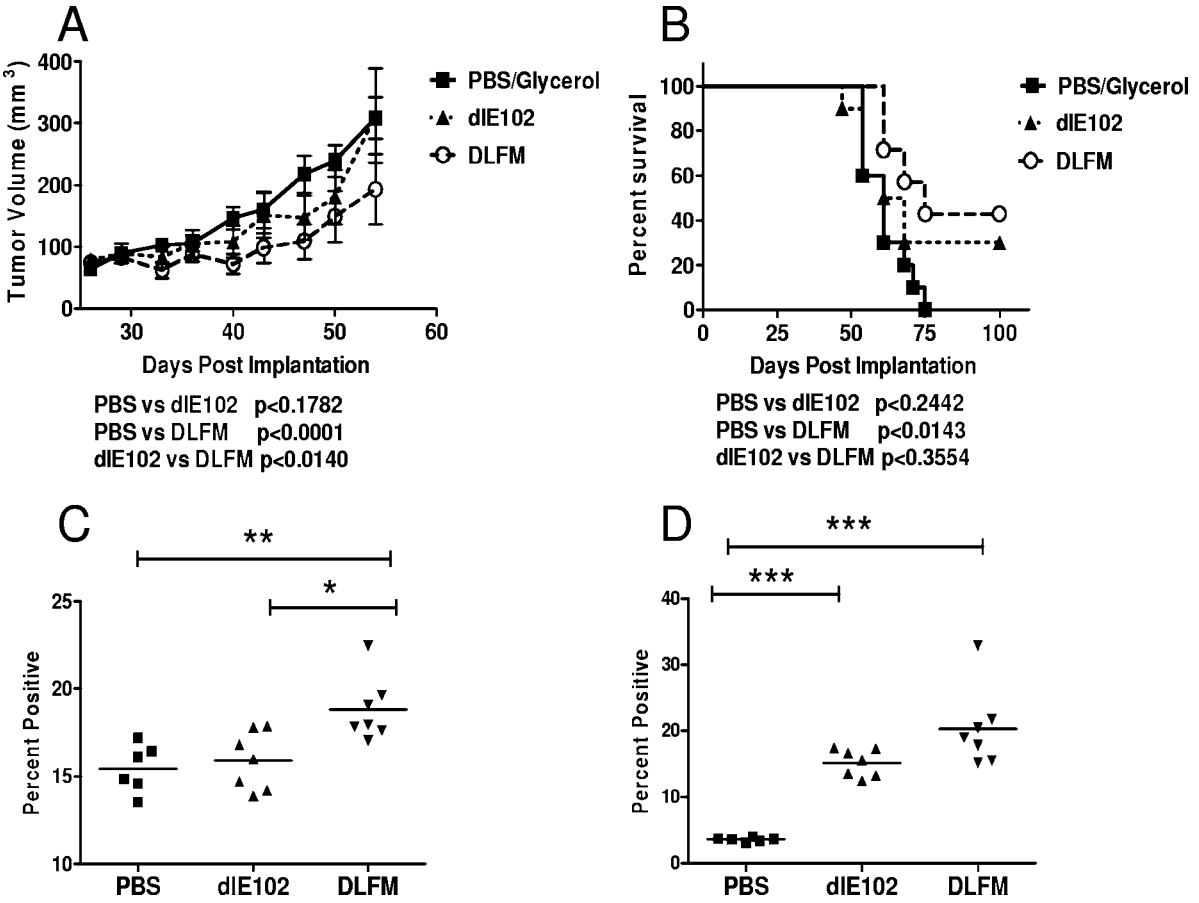

FIG. 7. Antitumor activities of armed MAV-1 vectors in the weakly immunogenic Pan02 xenograft tumor model. The DLFM vector was injected into Pan02 tumor-bearing animals, and tumor progression (A) and overall survival (B) were determined. Female C57BL/6 mice bearing Pan02 tumors (~80 mm^3) were injected weekly i.t. with the vehicle (PBS–10% [vol/vol] glycerol, $n = 10$), *dl*E102 (1×10^7 PFU in a 50-μl volume, $n = 9$), or DLFM (1×10^7 PFU in a 50-μl volume, $n = 7$). Tumor volume (A) was determined by caliper measurement and expressed as the mean tumor volume (cubic millimeters plus the standard error of the mean). In a separate study, Pan02 tumor-bearing mice were injected with two doses a week apart and 10 days later the mice were euthanized. The spleens were harvested, and the splenocytes were phenotyped by direct antibody staining and FACS analysis (C and D). The levels of activated T cells ($CD44^{hi}/CD62L^{low}$) in both the $CD4^+$ (C) and $CD8^+$ (D) subpopulations were determined. Differences between groups were analyzed by a one-way ANOVA with a Bonferroni correction (*, $P < 0.5$; **, $P < 0.01$; ***, $P < 0.001$).

i.t. in the immunocompetent murine CT26 tumor model, resulting in the complete eradication of established tumors. Previous studies have evaluated human Ad5-based oncolytic vectors in immunocompetent xenograft models (24). However, that approach provides for a suboptimal model since the levels of virus replication and cytotoxicity of the human viruses in murine tumor cells are known to be lower than in human tumor cells (24).

Since several oncolytic adenoviral vectors that are currently in preclinical (49, 53) or clinical (20, 46) development have been armed with anticancer transgenes (e.g., GM-CSF) to increase virus potency, we evaluated whether the murine viruses could be similarly armed. Most adenoviral vector arming strategies involve gene replacement (27) or the use of splice acceptor sequences to link transgenes to endogenous viral genes (30, 51). Both of these approaches require detailed knowledge of viral gene functions and transcription maps, neither of which has been fully defined for the MAV-1 genome. Therefore, a novel approach was used to arm *dl*E102, utilizing a furin cleavage sequence and the FMDV-derived 2A self-processing peptide, which allows equimolar expression of two transgenes from a single promoter (16). The benefits of this approach were that (i) a transgene can be inserted either directly upstream or downstream of an endogenous viral gene, (ii) only minimal (100-bp) exogenous regulatory sequences need to be added, and (iii) only the actual coding sequence, not the function, of the viral gene needs to be defined. The expression kinetics of the transgene will mirror that of the endogenous gene.

*dl*E102 was armed with the mGM-CSF transgene by insertion of a furin-2A-containing GM-CSF expression cassette upstream (DMFL) or downstream (DLFM) of the MAV-1 L3 gene. The MAV-1 L3 gene is homologous to the human Ad5 23K gene that is expressed late during virus infection following DNA replication (51). Insertion of the transgene expression cassette downstream of L3 (DLFM) had no effect on virus growth and allowed a high level of transgene expression, both in vitro and in vivo, that was dependent on virus replication. Interestingly, when the transgene cassette was inserted up-

stream of the L3 gene it had a deleterious effect on virus growth. This could be due to the insertion having negative effects on transcription.

The DLFM vector was tested in immunocompetent syngeneic tumor models to determine whether the addition of the adjuvant mGM-CSF to an oncolytic virus enhanced its antitumor potency by inducing a systemic antitumor immune response. In the highly immunogenic CT26 tumor model (as indicated by the fact that spontaneous regression may occur in 10 to 20% of untreated tumor-bearing animals), repeat administration of either *dl*E102 or DLFM completely eradicated the tumors in >80% of the mice. In addition, mice that remained tumor free after injection with the unarmed *dl*E102 vector were protected from a subsequent rechallenge with a lethal dose of CT26 cells, suggesting that treatment with even the unarmed oncolytic virus *dl*E102 was sufficient to induce a systemic immune response strong enough to prevent the outgrowth of the tumor at a different location within the host. The lack of effect of adjuvant GM-CSF may have been due to the highly immunogenic nature of the CT26 tumor model (41) or to the fact that the oncolytic activity of the vector alone was sufficient to eradicate tumors in 70 to 80% of the animals. However, although the vector potencies of the unarmed and armed viruses were similar in the CT26 model, mice treated with DLFM demonstrated a slightly, but not significantly, stronger anti-CT26-specific immune response. The apparent trend toward increased tumor-specific immune activation after DLFM injections was evident by four independent measures, suggesting that the adjuvant GM-CSF was able to enhance tumor-specific immune responses activated by the oncolytic virus.

Interestingly, the antitumor activities of *dl*E102 and DLFM were different in the weakly immunogenic Pan02 tumor model (38), in which DLFM treatment significantly reduced tumor growth compared to the PBS control group, in contrast to *dl*E102, which did not. The control of tumor growth in the DFLM-injected animals correlated with a strong increase in activated $CD4^+$ and $CD8^+$ T cells in the periphery. Thus, arming oncolytic adenovirus vectors with the immunomodulatory cytokine GM-CSF may enhance virus potency in weakly immunogenic tumor models compared to that of unarmed oncolytic viruses.

The development of an anti-adenovirus immune response is believed to be one of the reasons for the relatively mild efficacy often seen with oncolytic adenoviral vectors in clinical development. Neutralizing antibodies to adenovirus are believed to block readministration of the virus and thus lower its activity (47). The MAV-1 system provides for an ideal model to (i) examine the effects of anti-adenovirus specific immune responses on overall virus potency since the mice are immunocompetent and (ii) allow the evaluation of the effects of immunomodulatory therapies such as combination of anti-CTLA4 or anti-41BB with oncolytic virus therapy. These immune checkpoint regulators have been shown to significantly enhance the therapeutic benefit provided by cellular cancer immunotherapies (42, 56). As with many murine models, there are also limitations to the MAV-1 system that should be taken into account when using it as a homologous system to evaluate the mechanism of action of Ad5-based oncolytic vectors in immunocompetent hosts. As mentioned above, the natural host cells for MAV-1 are endothelial cells whereas for Ad5 the target cells are primarily respiratory epithelial cells. While there are recent studies that indicate that MAV-1 utilizes α_v integrin and heparin sulfate as receptors, similar to Ad5 (48), it does not use the CAR receptor for cellular attachment that is used by Ad5-based viruses (39). Thus, the in vivo toxicity and biodistribution profiles of the MAV-1 and Ad5 vectors are expected to be different and this model may therefore not be optimal for evaluation of the safety of the vectors in vivo. Some of these shortcomings of the model may be reduced or eliminated with further modifications of the MAV-1 vectors. With the Ad5 fiber engineered in place of the MAV-1 fiber, the fiber-modified MAV-1 vector most likely will utilize the CAR receptor for cell attachment. This modification therefore has the potential to change the tropism of the modified virus to one that closely mirrors the tropism of human Ad5 strains. Furthermore, evaluation of other mouse adenovirus species (e.g., MAV-2 or -3) is warranted to evaluate whether mouse adenoviruses exist that have biological properties more like those of Ad5 strains than like those of MAV-1.

In summary, the studies presented here demonstrate that MAV-1 is a valuable model for the evaluation of oncolytic vectors in immunocompetent syngeneic tumor models. We also demonstrated that arming oncolytic adenoviral vectors with GM-CSF can enhance the activation of antitumor immune responses and that such armed oncolytic viruses are more potent than unarmed viruses in animals with weakly immunogenic tumors. The use of the 2A-furin technology for arming MAV-1 readily permits the generation of oncolytic viruses that express various transgenes, which can be effectively evaluated in vivo in murine syngeneic tumor models. This model should also allow the evaluation of combination therapies of oncolytic adenoviral vectors with immunomodulatory therapies that are currently being developed in order to potentially improve the overall antitumor potency of the viruses.

ACKNOWLEDGMENTS

We thank P. Working for critical reading of the manuscript. B. Batiste, J. Ho, T. Langer, S. Tanciongo, and A. Welton are gratefully acknowledged for their technical assistance.

This work was supported by NIH R01 AI023762 to K.R.S.

REFERENCES

1. **Alemany, R., C. Balague, and D. T. Curiel.** 2000. Replicative adenoviruses for cancer therapy. Nat. Biotechnol. **18:**723–727.
2. **Ball, A. O., M. E. Williams, and K. R. Spindler.** 1988. Identification of mouse adenovirus type 1 early region 1: DNA sequence and a conserved transactivating function. J. Virol. **62:**3947–3957.
3. **Beard, C. W., and K. R. Spindler.** 1996. Analysis of early region 3 mutants of mouse adenovirus type 1. J. Virol. **70:**5867–5874.
4. **Beard, C. W., and K. R. Spindler.** 1995. Characterization of an 11K protein produced by early region 3 of mouse adenovirus type 1. Virology **208:**457–466.
5. **Biederer, C., S. Ries, C. H. Brandts, and F. McCormick.** 2002. Replication-selective viruses for cancer therapy. J. Mol. Med. **80:**163–175.
6. **Blanke, C., C. Clark, E. R. Broun, G. Tricot, I. Cunningham, K. Cornetta, A. Hedderman, and R. Hromas.** 1995. Evolving pathogens in allogeneic bone marrow transplantation: increased fatal adenoviral infections. Am. J. Med. **99:**326–328.
7. **Bristol, J. A., M. Zhu, H. Ji, M. Mina, Y. Xie, L. Clarke, S. Forry-Schaudies, and D. L. Ennist.** 2003. In vitro and in vivo activities of an oncolytic adenoviral vector designed to express GM-CSF. Mol. Ther. **7:**755–764.
8. **Carrigan, D. R.** 1997. Adenovirus infections in immunocompromised patients. Am. J. Med. **102:**71–74.
9. **Cauthen, A., and K. Spindler.** 1999. Construction of mouse adenovirus type 1 mutants, p. 85–103. *In* W. S. M. Wold (ed.), Adenovirus methods and protocols, vol. 21. Humana Press, Inc., Totowa, NJ.

10. **Cauthen, A. N., and K. R. Spindler.** 1999. Novel expression of mouse adenovirus type 1 early region 3 gp11K at late times after infection. Virology **259:**119–128.
11. **Charles, P. C., J. D. Guida, C. F. Brosnan, and M. S. Horwitz.** 1998. Mouse adenovirus type-1 replication is restricted to vascular endothelium in the CNS of susceptible strains of mice. Virology **245:**216–228.
12. **Chartier, C., E. Degryse, M. Gantzer, A. Dieterle, A. Pavirani, and M. Mehtali.** 1996. Efficient generation of recombinant adenovirus vectors by homologous recombination in *Escherichia coli*. J. Virol. **70:**4805–4810.
13. **Dechecchi, M. C., P. Melotti, A. Bonizzato, M. Santacatterina, M. Chilosi, and G. Cabrini.** 2001. Heparan sulfate glycosaminoglycans are receptors sufficient to mediate the initial binding of adenovirus types 2 and 5. J. Virol. **75:**8772–8780.
14. **Dechecchi, M. C., A. Tamanini, A. Bonizzato, and G. Cabrini.** 2000. Heparan sulfate glycosaminoglycans are involved in adenovirus type 5 and 2-host cell interactions. Virology **268:**382–390.
15. **Eggerding, F. A., and W. C. Pierce.** 1986. Molecular biology of adenovirus type 2 semipermissive infections. I. Viral growth and expression of viral replicative functions during restricted adenovirus infection. Virology **148:**97–113.
16. **Fang, J., S. Yi, A. Simmons, G. H. Tu, M. Nguyen, T. C. Harding, M. VanRoey, and K. Jooss.** 2007. An antibody delivery system for regulated expression of therapeutic levels of monoclonal antibodies in vivo. Mol. Ther. **15:**1153–1159.
17. **Fang, L., and K. R. Spindler.** 2005. E1A-CR3 interaction-dependent and -independent functions of mSur2 in viral replication of early region 1A mutants of mouse adenovirus type 1. J. Virol. **79:**3267–3276.
18. **Flomenberg, P., J. Babbitt, W. R. Drobyski, R. C. Ash, D. R. Carrigan, G. V. Sedmak, T. McAuliffe, B. Camitta, M. M. Horowitz, N. Bunin, et al.** 1994. Increasing incidence of adenovirus disease in bone marrow transplant recipients. J. Infect. Dis. **169:**775–781.
19. **Fox, J. P., C. D. Brandt, F. E. Wassermann, C. E. Hall, I. Spigland, A. Kogon, and L. R. Elveback.** 1969. The virus watch program: a continuing surveillance of viral infections in metropolitan New York families. VI. Observations of adenovirus infections: virus excretion patterns, antibody response, efficiency of surveillance, patterns of infections, and relation to illness. Am. J. Epidemiol. **89:**25–50.
20. **Freytag, S. O., B. Movsas, I. Aref, H. Stricker, J. Peabody, J. Pegg, Y. Zhang, K. N. Barton, S. L. Brown, M. Lu, A. Savera, and J. H. Kim.** 2007. Phase I trial of replication-competent adenovirus-mediated suicide gene therapy combined with IMRT for prostate cancer. Mol. Ther. **15:**1016–1023.
21. **Fueyo, J., C. Gomez-Manzano, R. Alemany, P. S. Lee, T. J. McDonnell, P. Mitlianga, Y. X. Shi, V. A. Levin, W. K. Yung, and A. P. Kyritsis.** 2000. A mutant oncolytic adenovirus targeting the Rb pathway produces anti-glioma effect in vivo. Oncogene **19:**2–12.
22. **Ginsberg, H. S., L. L. Moldawer, P. B. Sehgal, M. Redington, P. L. Kilian, R. M. Chanock, and G. A. Prince.** 1991. A mouse model for investigating the molecular pathogenesis of adenovirus pneumonia. Proc. Natl. Acad. Sci. USA **88:**1651–1655.
23. **Guida, J. D., G. Fejer, L. A. Pirofski, C. F. Brosnan, and M. S. Horwitz.** 1995. Mouse adenovirus type 1 causes a fatal hemorrhagic encephalomyelitis in adult C57BL/6 but not BALB/c mice. J. Virol. **69:**7674–7681.
24. **Halldén, G., R. Hill, Y. Wang, A. Anand, T. C. Liu, N. R. Lemoine, J. Francis, L. Hawkins, and D. Kirn.** 2003. Novel immunocompetent murine tumor models for the assessment of replication-competent oncolytic adenovirus efficacy. Mol. Ther. **8:**412–424.
25. **Hartley, J. W., and W. P. Rowe.** 1960. A new mouse virus apparently related to the adenovirus group. Virology **11:**645–647.
26. **Hawkins, L. K., and T. Hermiston.** 2001. Gene delivery from the E3 region of replicating human adenovirus: evaluation of the E3B region. Gene Ther. **8:**1142–1148.
27. **Hawkins, L. K., L. Johnson, M. Bauzon, J. A. Nye, D. Castro, G. A. Kitzes, M. D. Young, J. K. Holt, P. Trown, and T. W. Hermiston.** 2001. Gene delivery from the E3 region of replicating human adenovirus: evaluation of the 6.7 K/gp19 K region. Gene Ther. **8:**1123–1131.
28. **He, T. C., S. Zhou, L. T. da Costa, J. Yu, K. W. Kinzler, and B. Vogelstein.** 1998. A simplified system for generating recombinant adenoviruses. Proc. Natl. Acad. Sci. USA **95:**2509–2514.
29. **Heise, C., T. Hermiston, L. Johnson, G. Brooks, A. Sampson-Johannes, A. Williams, L. Hawkins, and D. Kirn.** 2000. An adenovirus E1A mutant that demonstrates potent and selective systemic anti-tumoral efficacy. Nat. Med. **6:**1134–1139.
30. **Jin, F., P. J. Kretschmer, and T. W. Hermiston.** 2005. Identification of novel insertion sites in the Ad5 genome that utilize the Ad splicing machinery for therapeutic gene expression. Mol. Ther. **12:**1052–1063.
31. **Johnson, L., A. Shen, L. Boyle, J. Kunich, K. Pandey, M. Lemmon, T. Hermiston, M. Giedlin, F. McCormick, and A. Fattaey.** 2002. Selectively replicating adenoviruses targeting deregulated E2F activity are potent, systemic antitumor agents. Cancer Cell **1:**325–337.
32. **Kajon, A. E., C. C. Brown, and K. R. Spindler.** 1998. Distribution of mouse adenovirus type 1 in intraperitoneally and intranasally infected adult outbred mice. J. Virol. **72:**1219–1223.
33. **Ko, D., L. Hawkins, and D. C. Yu.** 2005. Development of transcriptionally regulated oncolytic adenoviruses. Oncogene **24:**7763–7774.
34. **Kojaoghlanian, T., P. Flomenberg, and M. S. Horwitz.** 2003. The impact of adenovirus infection on the immunocompromised host. Rev. Med. Virol. **13:**155–171.
35. **Kring, S. C., C. S. King, and K. R. Spindler.** 1995. Susceptibility and signs associated with mouse adenovirus type 1 infection of adult outbred Swiss mice. J. Virol. **69:**8084–8088.
36. **Kring, S. C., and K. R. Spindler.** 1996. Lack of effect of mouse adenovirus type 1 infection on cell surface expression of major histocompatibility complex class I antigens. J. Virol. **70:**5495–5502.
37. **Larsen, S. H., and D. Nathans.** 1977. Mouse adenovirus: growth of plaque-purified FL virus in cell lines and characterization of viral DNA. Virology **82:**182–195.
38. **Le, H. N., N. C. Lee, K. Tsung, and J. A. Norton.** 2001. Pre-existing tumor-sensitized T cells are essential for eradication of established tumors by IL-12 and cyclophosphamide plus IL-12. J. Immunol. **167:**6765–6772.
39. **Lenaerts, L., D. Daelemans, N. Geukens, E. De Clercq, and L. Naesens.** 2006. Mouse adenovirus type 1 attachment is not mediated by the coxsackie-adenovirus receptor. FEBS Lett. **580:**3937–3942.
40. **Lenaerts, L., E. Verbeken, E. De Clercq, and L. Naesens.** 2005. Mouse adenovirus type 1 infection in SCID mice: an experimental model for antiviral therapy of systemic adenovirus infections. Antimicrob. Agents Chemother. **49:**4689–4699.
41. **Li, B., A. S. Lalani, T. C. Harding, B. Luan, K. Koprivnikar, G. Huan Tu, R. Prell, M. J. VanRoey, A. D. Simmons, and K. Jooss.** 2006. Vascular endothelial growth factor blockade reduces intratumoral regulatory T cells and enhances the efficacy of a GM-CSF-secreting cancer immunotherapy. Clin. Cancer Res. **12:**6808–6816.
42. **Li, B., J. Lin, M. Vanroey, M. Jure-Kunkel, and K. Jooss.** 2007. Established B16 tumors are rejected following treatment with GM-CSF-secreting tumor cell immunotherapy in combination with anti-4-1BB mAb. Clin. Immunol. **125:**76–87.
43. **Lin, J. M., B. Li, E. Rimmer, M. VanRoey, and K. Jooss.** 2008. Enhancement of the anti-tumor efficacy of a GM-CSF-secreting tumor cell immunotherapy in preclinical models by cytosine arabinoside. Exp. Hematol. **36:**319–328.
44. **Moore, M. L., C. C. Brown, and K. R. Spindler.** 2003. T cells cause acute immunopathology and are required for long-term survival in mouse adenovirus type 1-induced encephalomyelitis. J. Virol. **77:**10060–10070.
45. **Moore, M. L., E. L. McKissic, C. C. Brown, J. E. Wilkinson, and K. R. Spindler.** 2004. Fatal disseminated mouse adenovirus type 1 infection in mice lacking B cells or Bruton's tyrosine kinase. J. Virol. **78:**5584–5590.
46. **Nemunaitis, J. J., J. M. McKiernan, D. L. Lamm, M. V. Meng, J. C. Arseneau, J. Stephenson, J. M. Burke, J. Aimi, and D. J. Maslyar.** 2008. Phase 1 study of multi-dose administration of intravesical CG0070 in patients with non-muscle invasive bladder cancer (NMIBC). Mol. Ther. **16:**S256.
47. **Post, L. E.** 2002. Selectively replicating adenoviruses for cancer therapy: an update on clinical development. Curr. Opin. Investig. Drugs **3:**1768–1772.
48. **Raman, S., T. H. Hsu, S. L. Ashley, and K. R. Spindler.** 28 January 2009. Integrin and heparan sulfate usage as receptors for mouse adenovirus type 1. J. Virol. doi:10.1128/JVI.02368-08.
49. **Ramesh, N., Y. Ge, D. L. Ennist, M. Zhu, M. Mina, S. Ganesh, P. S. Reddy, and D. C. Yu.** 2006. CG0070, a conditionally replicating granulocyte macrophage colony-stimulating factor-armed oncolytic adenovirus for the treatment of bladder cancer. Clin. Cancer Res. **12:**305–313.
50. **Reddy, P. S., S. Ganesh, and D. C. Yu.** 2006. Enhanced gene transfer and oncolysis of head and neck cancer and melanoma cells by fiber chimeric oncolytic adenoviruses. Clin. Cancer Res. **12:**2869–2878.
51. **Robinson, M., Y. Ge, D. Ko, S. Yendluri, G. Laflamme, L. Hawkins, and K. Jooss.** 2008. Comparison of the E3 and L3 regions for arming oncolytic adenoviruses to achieve a high level of tumor-specific transgene expression. Cancer Gene Ther. **15:**9–17.
52. **Rowe, W. P., and J. W. Hartley.** 1962. A general review of the adenoviruses. Ann. N. Y. Acad. Sci. **101:**466–474.
53. **Sarkar, D., Z. Z. Su, and P. B. Fisher.** 2006. Unique conditionally replication competent bipartite adenoviruses-cancer terminator viruses (CTV): efficacious reagents for cancer gene therapy. Cell Cycle **5:**1531–1536.
54. **Schaack, J.** 2005. Induction and inhibition of innate inflammatory responses by adenovirus early region proteins. Viral Immunol. **18:**79–88.
55. **Silverstein, G., and W. A. Strohl.** 1986. Restricted replication of adenovirus type 2 in mouse Balb/3T3 cells. Arch. Virol. **87:**241–264.
56. **Simmons, A. D., M. Moskalenko, J. Creson, J. Fang, S. Yi, M. J. VanRoey, J. P. Allison, and K. Jooss.** 2008. Local secretion of anti-CTLA-4 enhances the therapeutic efficacy of a cancer immunotherapy with reduced evidence of systemic autoimmunity. Cancer Immunol. Immunother. **57:**1263–1270.
57. **Smith, K., C. C. Brown, and K. R. Spindler.** 1998. The role of mouse adenovirus type 1 early region 1A in acute and persistent infections in mice. J. Virol. **72:**5699–5706.
58. **Smith, K., B. Ying, A. O. Ball, C. W. Beard, and K. R. Spindler.** 1996. Interaction of mouse adenovirus type 1 early region 1A protein with cellular proteins pRb and p107. Virology **224:**184–197.
59. **Spindler, K. R., M. L. Moore, and A. N. Cauthen.** 2007. Mouse adenovirus,

p. 49–65. *In* J. Fox, S. Barthold, M. Davisson, C. Newcomer, F. Quimby, and A. Smith (ed.), The mouse in biomedical research, 2nd ed., vol. II. Academic Press, Inc., New York, NY.

60. **Thomas, M. A., J. F. Spencer, M. C. La Regina, D. Dhar, A. E. Tollefson, K. Toth, and W. S. Wold.** 2006. Syrian hamster as a permissive immunocompetent animal model for the study of oncolytic adenovirus vectors. Cancer Res. **66:**1270–1276.
61. **Toth, K., J. F. Spencer, A. E. Tollefson, M. Kuppuswamy, K. Doronin, D. L. Lichtenstein, M. C. La Regina, G. A. Prince, and W. S. Wold.** 2005. Cotton rat tumor model for the evaluation of oncolytic adenoviruses. Hum. Gene Ther. **16:**139–146.
62. **van der Veen, J., and A. Mes.** 1973. Experimental infection with mouse adenovirus in adult mice. Arch. Gesamte Virusforsch. **42:**235–241.
63. **Warrens, A. N., M. D. Jones, and R. I. Lechler.** 1997. Splicing by overlap extension by PCR using asymmetric amplification: an improved technique for the generation of hybrid proteins of immunological interest. Gene **186:** 29–35.
64. **Weinberg, J. B., G. S. Stempfle, J. E. Wilkinson, J. G. Younger, and K. R. Spindler.** 2005. Acute respiratory infection with mouse adenovirus type 1. Virology **340:**245–254.
65. **Wickham, T. J., P. Mathias, D. A. Cheresh, and G. R. Nemerow.** 1993. Integrins $\alpha_v\beta_3$ and $\alpha_v\beta_5$ promote adenovirus internalization but not virus attachment. Cell **73:**309–319.
66. **Wold, W. S., and M. S. Horwitz.** 2007. Adenoviruses, p. 2395–2436. *In* D. M. Knipe and P. M. Howley (ed.), Fields virologyt, vol. 2. Lippincott Williams & Wilkins, Philadelphia, PA.
67. **Ying, B., K. Smith, and K. R. Spindler.** 1998. Mouse adenovirus type 1 early region 1A is dispensable for growth in cultured fibroblasts. J. Virol. **72:**6325–6331.